Toward a systematic nucleus-nucleus potential for peripheral collisions

Y. P. Xu and D. Y. Pang*

School of Physics and Nuclear Energy Engineering, Beihang University, Beijing, 100191, China

(Received 4 February 2013; revised manuscript received 18 March 2013; published 8 April 2013)

A systematic nucleus-nucleus potential is proposed based on an optical model analysis of angular distributions of differential cross sections of ^{6}Li and ^{7}Li elastic scattering from targets with $A \geqslant 40$ with incident energies between 5 and 40 MeV/nucleon. A single-folding model based on the Bruyères Jeukenne-Lejeune-Mahaux (JLMB) model nucleon-nucleus potentials was used. Systematics in energy dependence of the potential parameters were obtained. This systematics was found to give reasonable account for both elastic scattering and total reaction cross sections for projectiles with mass numbers up to $A \sim 40$, including both stable and unstable nuclei, for incident energies from the vicinity of the Coulomb barrier to about 100 MeV/nucleon.

DOI: 10.1103/PhysRevC.87.044605 PACS number(s): 24.10.Ht, 25.10.+s, 25.70.Bc

I. INTRODUCTION

Systematics in optical model potentials are extremely important in describing nuclear reactions. Systematic optical model potentials not only allow people to study nuclear reactions consistently [1], they are also essential in studies of nuclear reactions induced by radioactive nuclei. Unlike light particles; namely, proton, neutron, deuteron, helion, triton, and alpha-particle for which many studies have been made on systematics of their optical potentials [2–9], studies on systematics of nucleus-nucleus (AA) potentials (with $A \geqslant 6$) are very rare. For many years the only published results were for ^{6}Li and ^{7}Li [10]. The reason is not only because there are much fewer experimental data for heavy ions than for light particles. Nuclear reactions induced by heavy ions are also more complicated than those involving light particles. Complicated reaction dynamics are involved, such as strong collective excitations, breakup, and transfer reactions [11] in heavy-ion reactions. However, recently considerable progress has been made on systematic AA potentials. By taking into account the Pauli nonlocality of the nucleon potentials and a parameterized nuclear densities, Chamon *et al*. proposed a global description of the nucleus-nucleus interactions (the São Paulo potential, SPP) [12]. Considerable success has been obtained when applying this systematic potential to various cases including both stable and unstable particles [13,14]. Recently, another global AA potential, which covers a large range of nuclear masses and for incident energies above 50 MeV/nucleon, with a complex G-matrix interaction and the São Paulo systematics of nuclear density were proposed by Furumoto *et al*. [15].

In this paper, we propose to study the global nucleus-nucleus potential with a single-folding model (SFM) approach. With this model, a nucleon potential, which is responsible to the nucleon-nucleus elastic scattering and total reaction cross sections, is folded with the nucleon density distribution of the projectile nucleus. The single-folded AA potential is then renormalized by fitting the nucleus-nucleus elastic scattering data. One important property of the SFM is that it connects the properties of simple systems, the nucleon-nucleus potential, to that of a complex systems, the AA potential. The resulting renormalization factors (RFs) of the AA potential could be studied theoretically. Perkin, Kobos, and Rook attribute the real parts of the RFs and their energy dependence to (i) three-body terms, (ii) the Pauli principle, and (iii) the energy dependence of the nucleon-nucleus potential [16] (the PKR model), which quantitatively agrees with the empirical results for deuteron, ^{3}He, and ^{4}He [9,16]. The renormalization factors can also be related to the nonlocality of the nucleon-nucleus potentials [17]. Understanding of these properties are important in nuclear physics. In this work we aimed not only to study the systematics of the heavy-ion potential but also to provide the "experimental data" for further theoretical studies on their renormalization factors.

The single-folding-model approach has been previously used to study the systematics of deuteron and alpha-particle potentials [9,18]. In this paper we apply the same method to the ^{6}Li and ^{7}Li potentials. Experimental angular distributions of elastic scattering cross sections are fit and optimum renormalization factors for each data set are obtained, from which the energy dependence of these RFs are derived. Unexpectedly, the resulting systematics was found to account well for elastic scattering of not only ^{6}Li and ^{7}Li themselves, but also for the elastic scattering and total reaction cross sections of much heavier projectiles with mass numbers up to $A = 40$, including both stable and unstable nuclei. This result suggests that a systematic AA potential can be obtained with the single-folding-model approach. Detailed descriptions of the procedures are presented in this paper.

This paper is organized as follows: the single-folding model for nucleus-nucleus potentials is briefly introduced in Sec. II. Details of the analysis of the experimental data are given in Sec. III. The energy dependence of the renormalization factors for the real and imaginary potentials are obtained and examined with the angular distributions (ADs) of elastic scattering cross sections and total reaction cross sections (σ_R) for various projectiles at different incident energies. The sensitivity of the nucleus-nucleus elastic scattering cross sections and their total reaction cross sections to the potential parameters are also investigated in this section.

*dypang@buaa.edu.cn

Discussions of the results and conclusions are given in Sec. IV.

II. SINGLE-FOLDING MODEL OF NUCLEUS-NUCLEUS POTENTIAL

With the single-folding model the nuclear potential encountered by a projectile nucleus (P) in its collision with a target nucleus (T) at incident energy $E_{\rm lab}$ is

$$U_{\rm SF}(R, E_{\rm lab}) = \sum_{i=p,n} \int \rho_i^P(\boldsymbol{r}) U_{i\rm T}(|\boldsymbol{s}|, E_i) d\boldsymbol{r}, \qquad (1)$$

where $\boldsymbol{R}$ is the vector from the center of mass (c.m.) of the target nucleus to that of the projectile; $\rho_i^P(\boldsymbol{r})$ is the nucleon ($i = p$ for proton and $i = n$ for neutron) density in the projectile at position $\boldsymbol{r}$ from its center of mass, and $\boldsymbol{s}$ is $\boldsymbol{R} + \boldsymbol{r}$; $U_{i\rm T}(|\boldsymbol{s}|, E_i)$, as a function of $|\boldsymbol{s}|$ and incident energy per nucleon of the projectiles, is the optical model potential for the nucleon-target system. In the single-folding model the NA potential should account for the elastic scattering of the nucleon from the target nucleus at the incident energy $E_i = E_{\rm lab}/A_p$. In this work we found it convenient to use the semimicroscopic Lane-consistent JLMB model potential [19,20] because, compared to phenomenological potentials, it allows the geometry (radii and diffuseness) of the resulting AA potential to vary with incident energy through its energy-dependent finite-range Gaussian parameters ($t_{\rm r}$ and $t_{\rm i}$, defined in, e.g., Refs. [19,20]) within a reasonable range [9,18]. Energy dependence in geometry of a systematic AA potential is important to describe the nucleus-nucleus elastic scattering within a sufficiently large range of incident energies [9]. Details of the calculations of $U_{i\rm T}$ have been given in Refs. [9,19,20] and are omitted in this paper.

Point proton and neutron density distributions of the projectile [in Eq. (1)] and the target nuclei (in calculating $U_{i\rm T}$ [19,20]) are required in the single-folding model for the AA potentials. In this work, results of the independent-particle model were used for the nucleon density distributions of ^{6}Li and ^{7}Li [21]. The corresponding root-mean-square radii are 2.401 and 2.367 fm for ^{6}Li and ^{7}Li, which are close to their experimental values of 2.43 ± 0.02 and 2.33 ± 0.02 fm, respectively [22]. Expect where explicitly stated, all proton and neutron density distributions in the target nuclei are obtained from Hartree-Fock (HF) calculations based on the SkX parametrization [23]. This parameter set accounts for the differences of binding energies for mirror nuclei [24], interaction cross sections [25], and nuclear charge distributions [26] and has been extensively used in folding-model calculations [9,27].

Equation (1) is only used for the calculation of the nuclear part of the nucleus-nucleus potential. The Coulomb potential has to be added for the full potential. Additionally, due to the compositeness of the projectile nucleus [16], its SFM potential has to be renormalized for describing its elastic scattering and total reaction cross sections with a target nucleus. So, eventually, a full AA potential in our single-folding-model approach takes the following form:

$$U(R, E_{\rm lab}) = N_{\rm r}{\rm Re}[U_{\rm SF}(R, E_{\rm lab})] + iN_{\rm i}{\rm Im}[U_{\rm SF}(R, E_{\rm lab})] + V_{\rm C}(R), \qquad (2)$$

where $N_{\rm r}$ and $N_{\rm i}$ are renormalization factors for the real and imaginary potentials, respectively. The Coulomb potential, $V_{\rm C}$, is calculated in the usual way with a radius $R_{\rm C} = r_{\rm C}(A_{\rm T}^{1/3} + A_{\rm P}^{1/3})$ where $r_{\rm C}$ is fixed to 1.3 fm. Both ^{6}Li and ^{7}Li have nonzero spins in their ground states. However, in this work, only angular distributions of elastic scattering cross sections were analyzed, which are known to be insensitive to spin-orbit potentials [28]. For this reason, spin-orbit potentials are not included in this work. In Ref. [9,18] we also study the energy dependence of the finite-range Gaussian parameters $t_{\rm r}$ and $t_{\rm i}$ [19,20]. That approach was necessary for a range of incident energies between 10 and 100 MeV/nucleon (see Fig. 2 in Ref. [9]). The energy range analyzed in the present work is only between 5 and 40 MeV/nucleon, within which the $t_{\rm r}$ and $t_{\rm i}$ values can be taken to be constants. In this work, we keep their values to be $t_{\rm r} = 1.25$ fm and $t_{\rm i} = 1.35$ fm, which, overall, provide good systematic nucleon-nucleus potential for various targets from 1 keV to about 200 MeV [19,20].

III. DATA ANALYSIS

A. Derivation of systematic potential

The experimental data and their references are listed in Tables I and II. Only data on heavy targets were used. The incident energies included are between 5 and 40 MeV/nucleon. The upper limit is mainly due to the availability of the experimental data. All the experimental data were taken from the nuclear reaction database EXFOR/CSISRS [29], expect for ^{6}Li at 50.6, 99, and 156 MeV, and ^{7}Li at 52 and 88 MeV, which were digitized from the Refs. [30–33].

The computer code JLM was adapted for calculations of the JLMB model nucleon-nucleus potentials. Renormalization factors $N_{\rm r}$ and $N_{\rm i}$ were found by fitting experimental data with the standard minimum χ^2 (divided by the number of data points) method. Experimental error bars were used in these fits if they were available; otherwise, uniform uncertainties of 10% were applied for all data points. The optical model fittings were performed by using the computer code SFRESCO, which is a combination of the computer code FRESCO [34] and a parameter-search routine MINUIT [35]. Detailed descriptions for the procedure in the data analysis can be found in Ref. [9]. The resulting single-folding parameters are listed in Tables I and II for ^{6}Li and ^{7}Li, respectively, and are represented by the symbols in Fig. 1.

As we can see, within the energy range of 5 to 40 MeV/nucleon, the $N_{\rm r}$ values for ^{6}Li obtained from optical model fits to each individual data set can be represented by a linear function of incident energy, while the $N_{\rm i}$ values do not show an obvious energy dependence. Based on this observation, we fit $N_{\rm r}$ of ^{6}Li with a linear function, as shown in Eq. (3), and take $N_{\rm i}$ as a constant whose values was taken to be the average of the individually fit values, as is shown in Eq. (4). For ^{7}Li, the maximum incident energy analyzed is only 88 MeV. Within such small energy range, both $N_{\rm r}$ and $N_{\rm i}$ can be taken as constants, whose values are given in Eqs. (5) and (6). Note, however, that the distributions of $N_{\rm r}$ and $N_{\rm i}$ values of ^{7}Li overlap with those of ^{6}Li at the same energy range. We assume that they depend the same way on incident energy as those of

TABLE I. Experimental data analyzed in this work, their references, and their results of individual fittings for ^{6}Li. Note that the χ^2 values in this table are calculated with the energy-dependent potential derived in this work [Eqs. (3) and (4)].

Target	$E_{\rm lab}$/MeV	$N_{\rm r}$	$N_{\rm i}$	χ^2	Ref.
^{40}Ca	99.0	0.4688	1.223	17.7	[31]
	156.0	0.5426	1.275	18.1	[32]
	210.0	0.6960	1.474	53.7	[36]
	240.0	0.6472	1.345	29.2	[37]
^{48}Ca	240.0	0.6144	1.227	25.3	[37]
^{58}Ni	34.0	0.5341	1.650	1.02	[38]
	73.7	0.4604	1.202	8.38	[39]
	90.0	0.5367	1.097	48.1	[40]
	99.0	0.4746	1.164	23.1	[31]
	240.0	0.5018	1.262	38.6	[37]
^{89}Y	60.0	0.5560	1.213	7.51	[41]
^{90}Zr	70.0	0.5101	1.166	1.37	[42]
	73.7	0.3816	0.972	3.66	[39]
	99.0	0.4186	1.112	8.89	[31]
	210.0	0.6034	1.508	112	[36]
	240.0	0.6107	1.398	42.4	[37]
^{92}Zr	70.0	0.5118	0.995	8.88	[42]
^{94}Zr	70.0	0.5207	1.009	9.99	[42]
^{96}Zr	70.0	0.4939	0.968	8.60	[42]
^{116}Sn	240.0	0.5719	1.416	184	[43]
^{120}Sn	44.0	0.2394	1.022	6.57	[44]
	90.0	0.2673	7.741	13.8	[40]
^{124}Sn	73.7	0.4067	1.021	1.12	[39]
^{144}Sm	30.1	0.4095	1.837	1.78	[45]
	32.2	0.4452	1.683	1.22	[45]
	35.1	0.4278	1.816	0.969	[45]
	42.3	0.4173	1.304	1.85	[45]
^{208}Pb	31.0	0.3998	2.298	2.09	[46]
	33.0	0.3830	1.763	0.272	[47]
	35.0	0.3913	1.554	2.30	[46]
	39.0	0.4952	1.184	1.20	[47]
	50.6	0.3494	1.015	1.33	[30]
	73.7	0.4198	1.045	0.219	[39]
	90.0	0.8807	1.877	9.63	[40]
	99.0	0.4746	1.432	3.99	[31]
	156.0	0.6224	1.245	39.8	[32]
	210.0	0.4119	1.225	30.8	[36]
^{209}Bi	32.8	0.3803	1.681	0.160	[48]
	36.0	0.2850	2.029	2.41	[49]
	40.0	0.3223	1.826	8.24	[49]

^{6}Li. Note that the χ^2 values (divided by number of data points) in Tables I and II and the solid curves in Figs. 2 and 3 were obtained with the energy-dependent potential parameters in Eqs. (3) and (4). Note also that in order to compare the degree of agreement between different data sets, uniformly 10% of experimental uncertainties were assumed for all data sets when calculating the χ^2 values in Tables I and II. One sees that the systematic parameters can reproduce the ^{6}Li and ^{7}Li elastic scattering satisfactorily except for ^{6}Li elastic scattering at above 156 MeV. The uncertainties of $N_{\rm r}$ and $N_{\rm i}$ in Eqs. (3)–(6) are standard deviations of the differences between the individual values of these renormalization factors and their systematic

TABLE II. Same as Table I but for ^{7}Li.

Target	$E_{\rm lab}$/MeV	$N_{\rm r}$	$N_{\rm i}$	χ^2	Ref.
^{40}Ca	34.0	0.5806	1.390	22.7	[50]
	88.0	0.4281	1.059	23.1	[51]
^{44}Ca	34.0	0.4631	1.219	11.3	[50]
^{48}Ca	34.0	0.4471	1.217	5.76	[50]
	88.0	0.4257	1.030	46.7	[51]
^{54}Fe	36.0	0.5514	1.423	0.693	[50]
^{54}Fe	42.0	0.4596	1.255	0.952	[50]
^{54}Fe	48.0	0.4119	1.005	5.24	[50]
^{56}Fe	34.0	0.4658	1.192	2.00	[50]
^{58}Ni	34.0	0.5510	1.624	2.07	[50]
	42.0	0.3695	1.207	4.78	[52]
^{60}Ni	34.0	0.8040	2.023	3.11	[50]
^{89}Y	60.0	0.2799	0.969	3.58	[41]
^{90}Zr	34.0	0.5674	1.770	0.451	[50]
^{118}Sn	48.0	0.5726	1.290	2.11	[10]
^{144}Sm	35.0	0.4825	1.738	1.21	[45]
	40.8	0.3783	3.080	4.93	[45]
	52.0	0.6762	1.134	4.28	[33]
^{208}Pb	33.0	0.4032	0.689	1.45	[47]
	39.0	0.5960	1.939	6.03	[47]
	42.0	0.4023	1.266	0.089	[53]
	52.0	0.6470	1.316	2.86	[54]

values:

$$N_{\rm r}^{^{6}{\rm Li}}(E_{\rm lab}) = (0.00424E_{\rm lab}/A_{\rm P} + 0.423) \pm 0.068, \quad (3)$$

$$N_{\rm i}^{^{6}{\rm Li}} = 1.22 \pm 0.17, \quad (4)$$

$$N_{\rm r}^{^{7}{\rm Li}} = 0.489 \pm 0.096, \quad (5)$$

$$N_{\rm i}^{^{7}{\rm Li}} = 1.28 \pm 0.22. \quad (6)$$

Studies of ^{6}Li elastic scattering from ^{12}C show that the dynamic polarization potentials (DPPs) induced by projectile breakup couplings are oscillatory in regions when two nuclei are close to each other [55]. For such cases, the effect of DPP cannot be represented by overall renormalization factors over all radial ranges. For example, we see from Fig. 3 that the global potential parameters do not account well for the angular distributions of ^{6}Li at 156, 210, and 240 MeV at large angles, where the phenomena of rainbow scattering occurs, which is well known to be sensitive to the inner part of the optical model potentials [56]. Fortunately, as discussed in Ref. [57], typical elastic scattering data of heavy ions primarily determine the optical model potential near the strong absorption radius where the nuclear matter densities of the pair of colliding nuclei barely overlap [57]. This is true even for cases with rather high incident energies, such as ^{16}O elastic scattering at 94 MeV/nucleon, when the target nucleus is heavy ($A \geqslant 40$) so that the Coulomb force is strong [58]. For such peripheral collisions the systematic in RFs of single-folding potentials should apply. Actually, from Fig. 3 we also see that the magnitudes and shapes of angular distributions for center-of-mass angles smaller than the rainbow angles are well reproduced. This result suggest that the single-folding

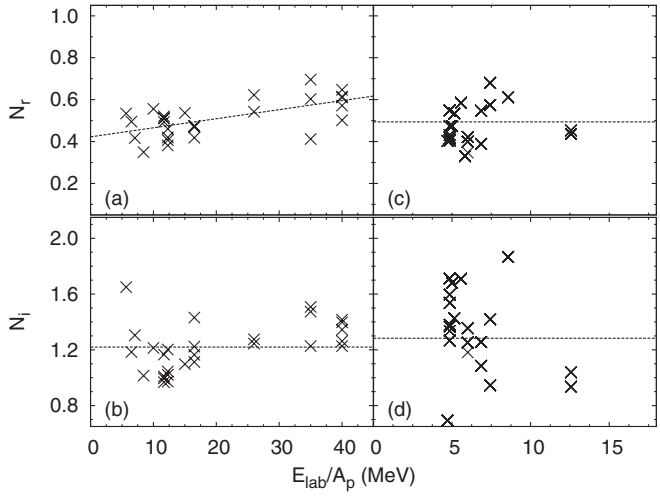

FIG. 1. N_r and N_i values from individual fits for ^{6}Li and ^{7}Li: (a) N_r for ^{6}Li, (b) N_i for ^{6}Li, (c) N_r for ^{7}Li, and (d) N_i for ^{7}Li. Their numerical values are shown in Tables I and II. The dashed curves represent the energy dependence of these parameters given by Eqs. (3)–(6).

model adopted in this paper account well for the surface part of the nucleus-nucleus potential. We demonstrate this in the following subsection.

B. Examination of systematic potential

The systematics of renormalization factors in Eqs. (3) and (4) are first checked with the elastic scattering data of ^{6}Li and ^{7}Li, from which the systematic potential was derived. The results are shown in Figs. 2 and 3 (their corresponding χ^2 values are presented in Tables I and II). For comparison, calculations were also made with the systematic potential derived by Cook [10] (depicted in dashed curves). In order to see the angular distributions at higher energies more clearly, the scattering angles in both figures are translated from $\theta_{\rm c.m.}$ to $\Theta_{\rm c.m.}$ [9]:

$$\Theta_{\rm c.m.} = \left[1 + E_{\rm lab}^{1/4} e^{-\theta_{\rm c.m.}/w}\right]\theta_{\rm c.m.}, \tag{7}$$

where w was taken to be 30 degrees. The effect of these translations can be seen in Fig. 4 for the cases of ^{6}Li and ^{7}Li elastic scattering from various targets at 73.7 and 42 MeV, respectively. The detailed differences in angular distributions with this work and Cook's systematics can also be seen in this figure. In general, experimental data can be satisfactorily described.

Nucleus-nucleus OMPs at low energies (around or even below Coulomb barriers) are of great interest in studies of fusion reactions. Experimental data at low energies, however, are not included in the present systematic analysis. This is not only because the optical model potential at low

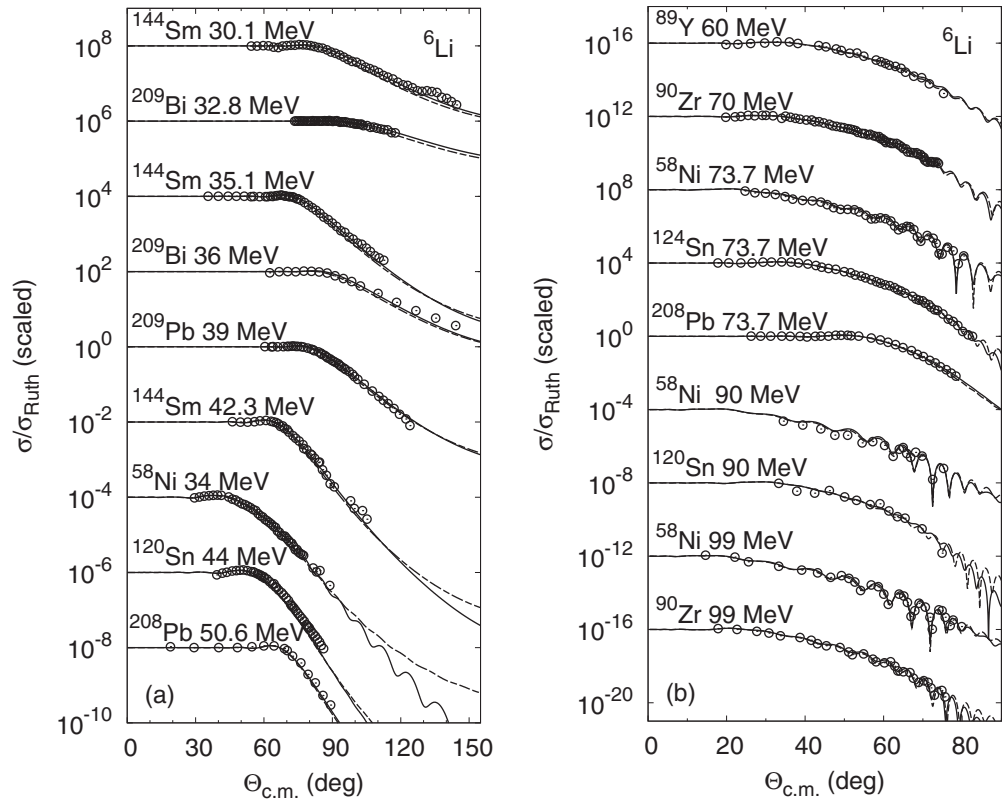

FIG. 2. Comparisons between optical model calculations and experimental data of ^{6}Li and ^{7}Li elastic scattering from heavy targets at incident energies indicated in the figures. The solid and dashed curves were calculated with the systematics in this work and that of Cook's [10], respectively. Different data sets are offset by factors of 100 in panel (a) and 10^4 in panel (b) for optimum view. Experimental error bar are smaller than size of the data points and are not shown in these figures.

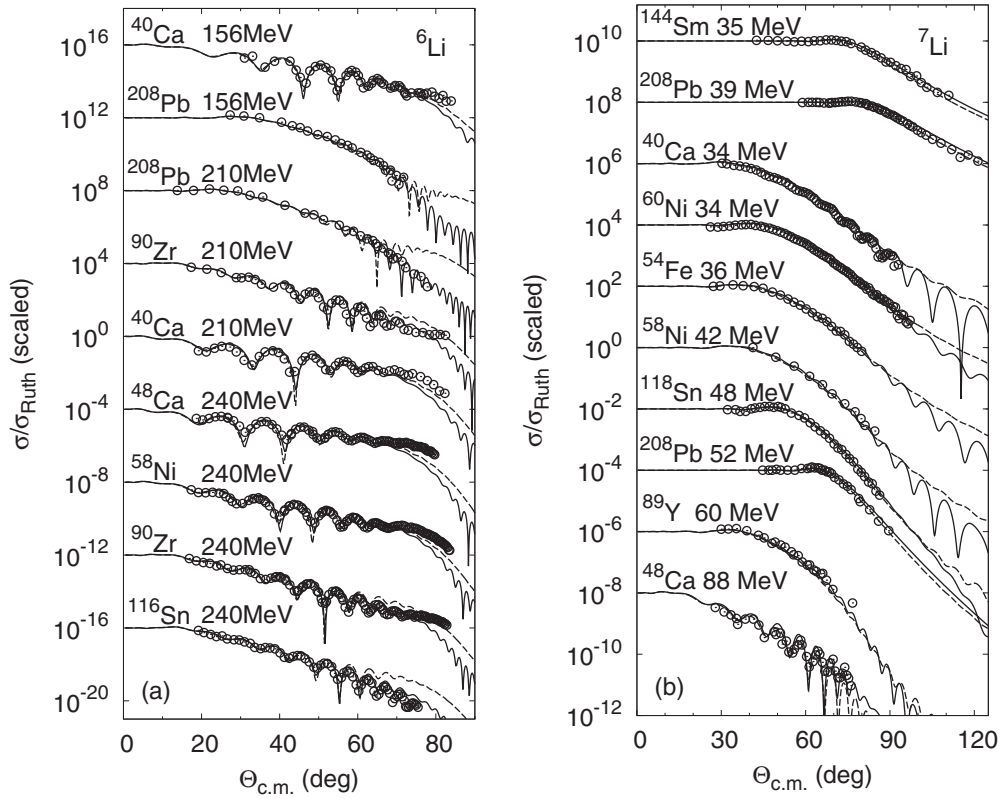

FIG. 3. Same as Fig. 2 but for ^{6}Li at higher incident energies (a) and for ^{7}Li (b).

energies suffer from greater uncertainties, but also because at incident energies near Coulomb barriers, the heavy-ion optical potentials show threshold anomaly, which cannot be represented by a simple linear function of incident energies [59]. It is interesting, phenomenologically, to see how a systematic potential derived from a high-energy region works when it is extrapolated to low-energy regions. In Fig. 5 we show results of optical model calculations for ^{6}Li and ^{7}Li elastic scattering from various targets at incident energies between 2 and 5 MeV/nucleon and their comparisons with the experimental data. Calculations with the SPP systematics are also shown as dashed curves. Although, in general, the present systematics reasonably reproduces these low-energy data and gives very close results to that of the SPP, for several cases it is inferior to the SPP by overestimating the differential cross sections at large angles (actually in those cases both systematics overestimate the cross sections). The reason may be because the Pauli nonlocality is especially

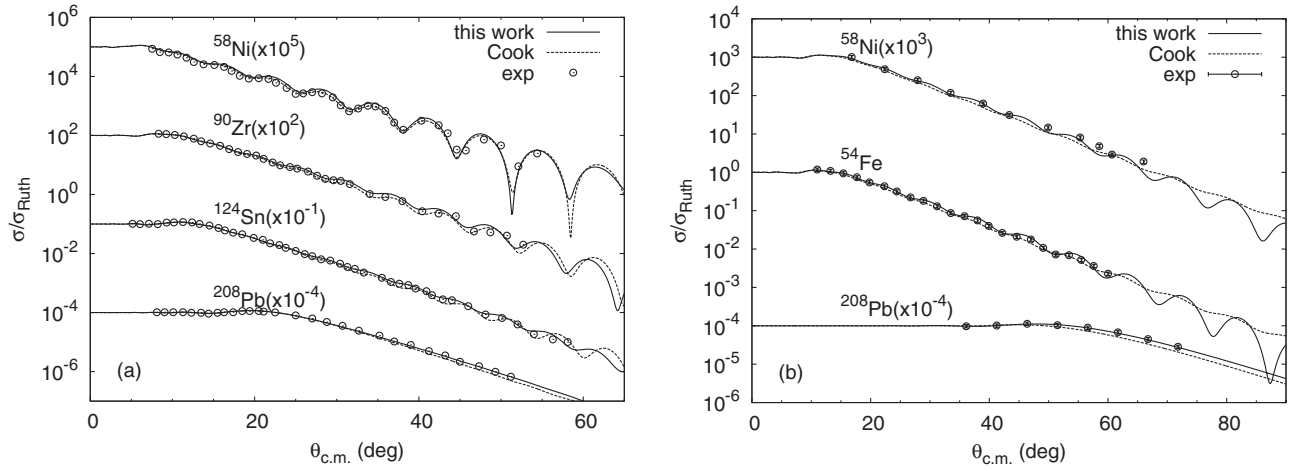

FIG. 4. Comparisons between optical model calculations and experimental data for (a) ^{6}Li elastic scattering at 73.7 MeV and (b) ^{7}Li elastic scattering at 42 MeV, respectively, from various targets. Note that $\theta_{\mathrm{c.m.}}$ is used in this figure instead of $\Theta_{\mathrm{c.m.}}$ to show the effect of the translation of the scattering angles and a more detailed view of the differences in the present systematics and Cook's systematics.

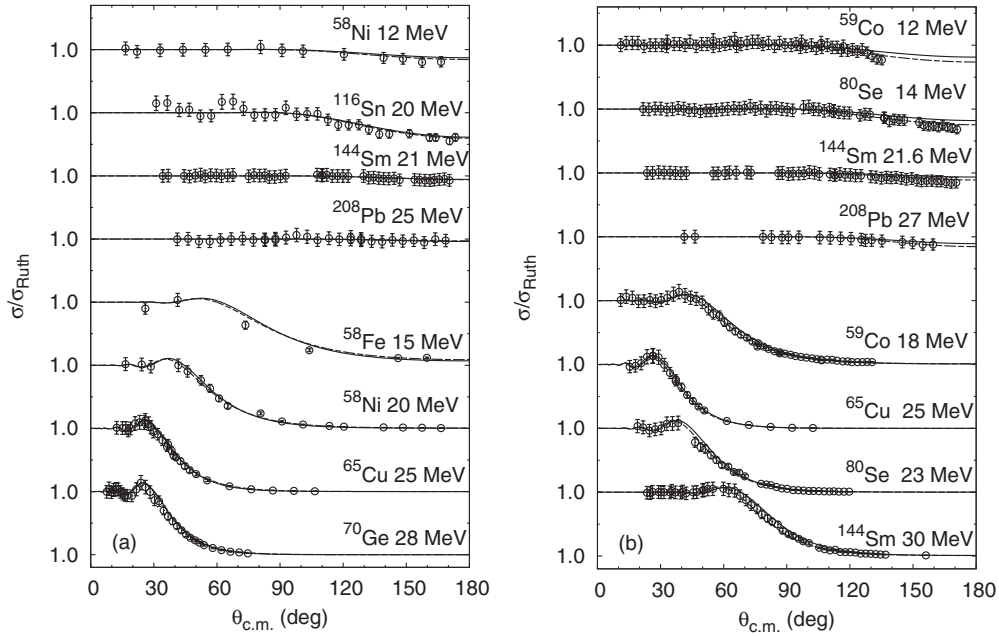

FIG. 5. Comparisons between the optical model calculations and experimental data for (a) ^{6}Li and (b) ^{7}Li elastic scattering from heavy targets at low energies ($E_{\rm lab} < 5$ MeV/nucleon). The incident energies are indicated in the figures. The solid and dashed curves were calculated with the present systematics and that of SPP, respectively. The data are plotted in linear scales. Uniform 10% uncertainties were assumed for all data points. The experimental data are all obtained from the EXFOR database with Refs. [45,46,61–69].

treated in SPP [60], which is important at low incident energies [16].

An important property of a systematic heavy-ion potential is its range of applicability with respect to projectile masses. In Figs. 6, 7, 8, and 9 we present the comparison between experimental data and optical model calculations for ^{12}C, ^{16}O, ^{32}S, and ^{40}Ar elastic scattering from various targets at incident energies from vicinity of Coulomb barrier to about 100 MeV/nucleon. These are the representatives of the stable nuclei we have checked with atomic masses between 6 and 40. The present systematics accounts well for the elastic scattering angular distributions for most of the cases we checked. Notice, however, that, it is not satisfactory for light targets with $A < 40$ (see, for example, ^{16}O elastic scattering from ^{12}C and ^{28}Si in Fig. 7). This, as discussed in Refs. [7,9,18], demonstrates that a systematics established from the heavy-target region does not guarantee the same quality of agreement for elastic scattering from light targets. Total reaction cross sections from optical model calculations using the present systematics also agree reasonably well with the experimental data. We take Fig. 10 as an example where σ_R for ^{12}C, ^{20}Ne, ^{40}Ar, and ^{40}Ca on various targets from $A = 12$ to $A = 208$ are shown. These results of optical model calculations are also close to those obtained with Kox's formula [70,71]. Except for ^{12}C, whose

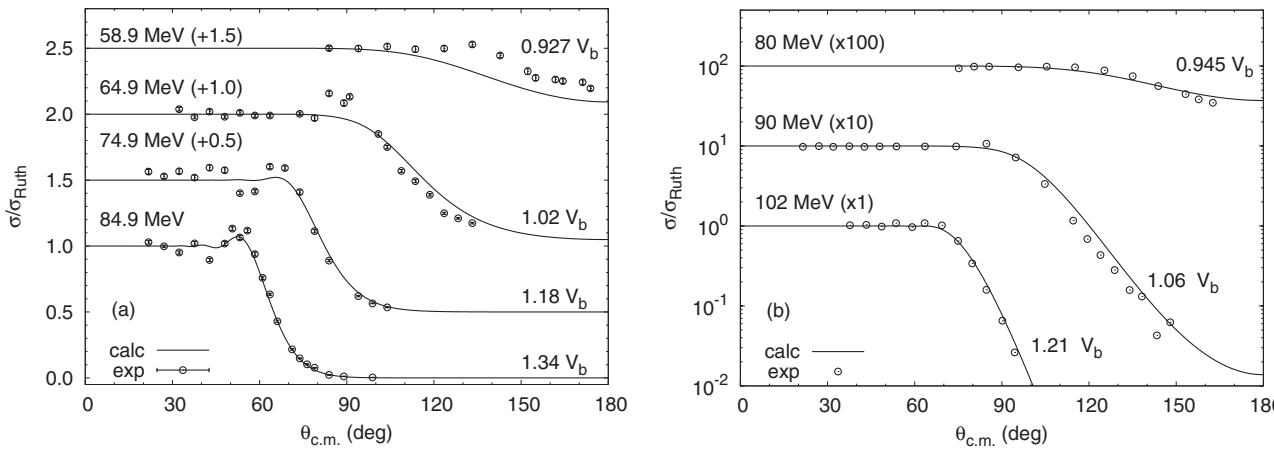

FIG. 6. Comparison between optical model calculations and experimental data for elastic scattering of (a) ^{12}C and (b) ^{16}O from ^{208}Pb at incident energies indicated in the figures with the systematic potential obtained in this work. The ratio between center-of-mass energies and the heights of Coulomb barriers (V_b) are also indicated in the figures. The experimental data are from Refs. [74,75].

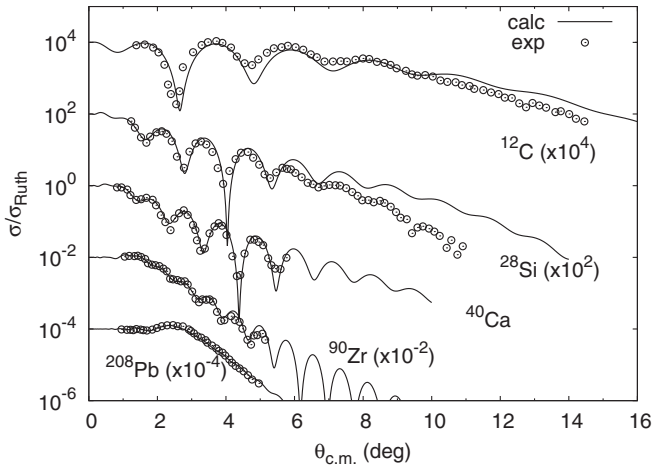

FIG. 7. Comparison between optical model calculations and experimental data for ^{16}O elastic scattering from various targets at 94 MeV/nucleon. The experimental data are from Ref. [58].

density distribution were taken to be a two-parameter Fermi function with parameters $\rho_0 = 0.194\ \mathrm{fm}^{-3}$, $c = 2.214$ fm, and $a = 0.425$ fm (set II in Table II of Ref. [72]), which has been extensively used in folding-model calculations [18,22]; the nucleon density distributions of other projectile are all taken from HF calculations using the SkX interaction as stated previously. Relativistic corrections [73] to the reaction kinematics were made for cases with incident energies above 40 MeV/nucleon, which was found to be necessary to reproduce the angular distributions of the elastic scattering cross sections on heavy targets.

For applying the present systematics to unstable nuclei, we found that it reproduces very well for ^{7}Be, ^{8}B [80], ^{10}C, and ^{11}C [81] the elastic scattering from ^{208}Pb at incident energies around three times the Coulomb barriers and ^{17}F elastic scattering from ^{208}Pb at 120 [82] and 170 MeV [83]. There are, however, no systematic measurements of elastic scattering

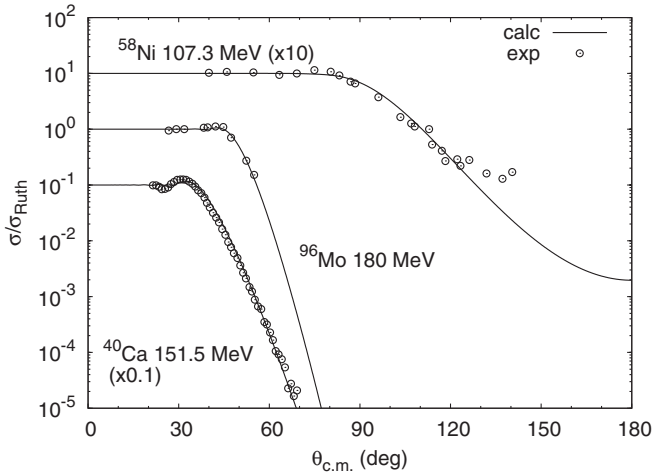

FIG. 8. Comparison between optical model calculations and experimental data for ^{32}S elastic scattering from various targets at incident energies indicated in the figure. The experimental data are from Refs. [76–78].

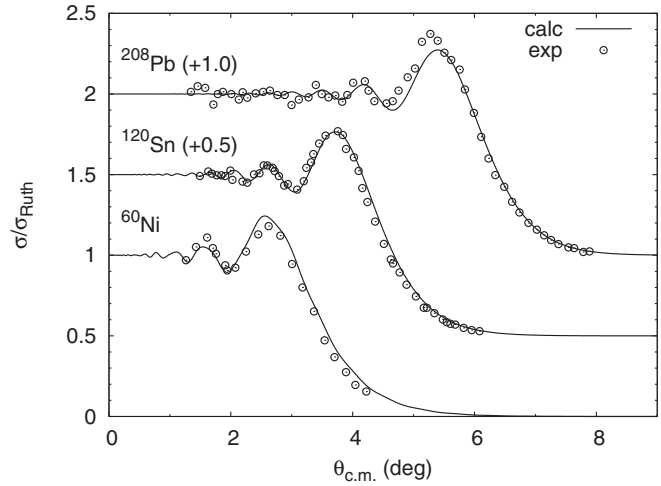

FIG. 9. Comparison between optical model calculations and experimental data for ^{40}Ar elastic scattering from ^{60}Ni, ^{120}Sn, and ^{208}Pb at 44 MeV/nucleon. The experimental data are from Ref. [79].

angular distributions for unstable nuclei to compare with. We demonstrate the applicability of the present systematics to unstable nuclei by comparison with their total reaction cross sections. Saint-Laurent *et al*. systematically measured the total reaction cross sections induced by Li, Be, B, C, N, O, and F isotopes including their neutron-rich ones on a natural copper target [84]. These data were analyzed by Liatard *et al*. to obtain the root-mean-square radii of the proton and neutron density distributions in those projectiles assuming Gaussian-form distributions [85]. We use these density distributions in our single-folding model calculations and apply the systematic

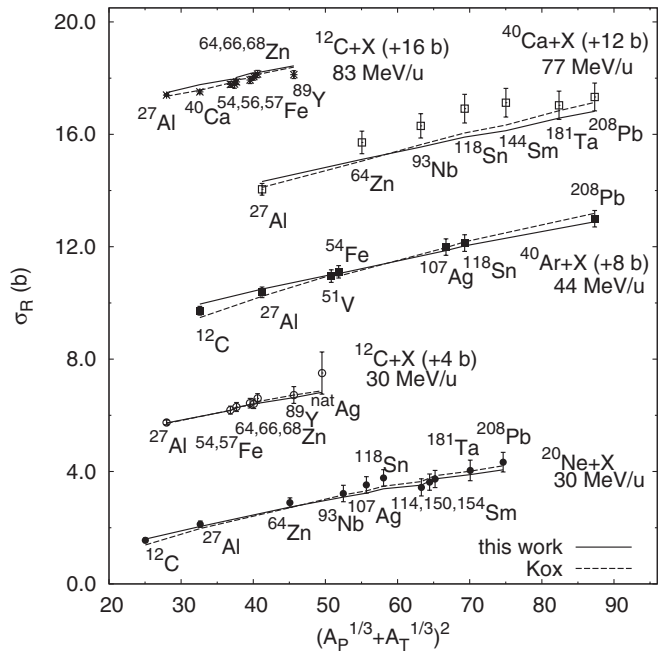

FIG. 10. Comparison between results of optical model calculations and experimental data for total reaction cross sections of ^{12}C, ^{20}Ne, ^{40}Ar and ^{40}Ca with various targets at incident energies indicated in the figure. The experimental data are from Refs. [70,86].

TABLE III. Total reaction cross sections of carbon isotopes on natural copper target at various energies and their comparisons with results of optical model calculations with the systematic potential. Their differences are denoted by $\Delta = |\sigma_R^{\rm expt} - \sigma_R^{\rm calc}|/\Delta\sigma_R^{\rm expt}$. The energies are in MeV/nucleon, and the total cross sections are in barn.

$A_{\rm P}$	$E_{\rm lab}$	$\sigma_R^{\rm expt} \pm \Delta\sigma_R^{\rm expt}$	$\sigma_R^{\rm calc}$	Δ
11	36.77	2.28 ± 0.44	2.35	0.169
12	29.78	2.404 ± 0.099	2.44	0.344
13	24.23	2.09 ± 0.13	2.47	2.935
	46.52	2.22 ± 0.35	2.39	0.498
14	19.78	1.88 ± 0.28	2.61	2.598
	39.52	2.521 ± 0.051	2.56	0.845
	45.00	2.62 ± 0.22	2.53	0.396
15	33.82	2.847 ± 0.59	2.72	0.213
	38.68	2.666 ± 0.081	2.70	0.354
16	29.10	2.69 ± 0.11	2.77	0.738
	33.44	2.743 ± 0.059	2.75	0.159
	44.64	2.19 ± 0.77	2.69	0.644
17	24.55	2.24 ± 0.51	2.99	1.466
	29.07	2.31 ± 0.20	2.98	3.324
	39.15	2.96 ± 0.12	2.92	0.366
18	34.51	2.89 ± 0.20	2.91	0.074
19	45.12	2.7 ± 1.5	2.78	0.053

renormalization factors to the resulting optical potentials. The resulting total reaction cross sections from optical model calculations are compared with experimental data for the $^{11-19}$C isotopes in Table III. The calculations agree with experimental data within experimental error bars with only a few exceptions. The same conclusion can be made for other isotopes reported in Ref. [84]. In these calculations proton and neutron density distribution of the natural copper target were taken to be the average of those of ^{63}Cu and ^{65}Cu, which were obtained with HF model calculations, weighted with their isotopic abundances.

The present systematic potential inevitably has limitations. As mentioned above, the systematics is not satisfactory for light targets with $A \lesssim 40$, such as ^{12}C and ^{28}Si. Limitations also exist in the optical model itself on which the systematic potential is based. We have checked that it cannot reproduce elastic scattering of exotic nuclei at around Coulomb barriers, such as ^{6}He + ^{208}Pb at 22 MeV [87] and ^{11}Be + ^{64}Zn at $E_{\rm c.m.} \simeq 24.5$ MeV [88]. Coupling effects from breakup reaction channels strongly suppress the Coulomb-nuclear interference peaks at intermediate angles for such cases [89]. Other couplings effects, such as strong Coulomb excitations, can also affect the elastic scattering angular distributions considerably [11]. The problem of strong Coulomb excitations become important when both projectile and target nuclei are heavy, which prohibits applying the present systematic potential to such cases. Examples can be seen in Fig. 11 where elastic scattering of ^{40}Ca and ^{86}Kr from ^{208}Pb at 235 and 695 MeV; both are close to their Coulomb barriers and are compared with optical model calculations with the systematic potential. The strong suppression of differential cross sections

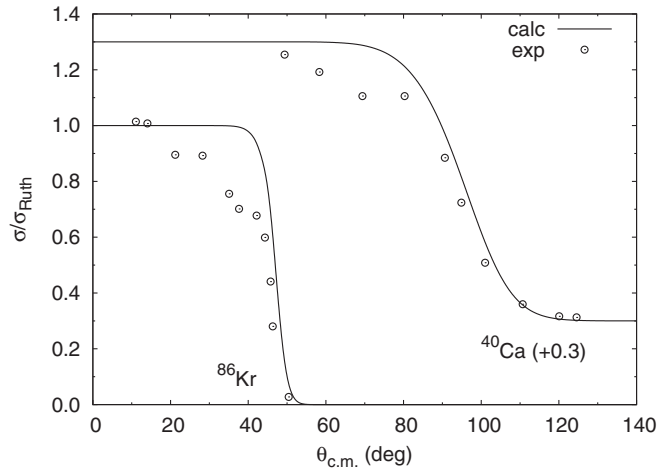

FIG. 11. Comparison between optical model calculations and experimental data for ^{40}Ca and ^{86}Kr elastic scattering from ^{208}Pb at around Coulomb barriers (235 and 695 MeV, respectively). The experimental data are from Refs. [90,91].

at intermediate angles in both cases cannot be reproduced by the optical model calculation with the systematic potential.

C. Sensitivity test of potential parameters

Many studies shows that the double-folding potentials of ^{6}Li and ^{7}Li have to be reduced by around 40%–50% to reproduce their elastic scattering data [92]. It was later found that this phenomena is related to the dynamic polarization potentials induced by couplings from continuum states of the projectiles due to their weakly bound nature [93]. Notice that the $N_{\rm r}$ values for ^{6}Li and ^{7}Li are also around 0.5 with the single-folding model adopted in this paper. One thus would expect that this is also due to the effects of breakup couplings to the elastic channel. However, it is then puzzling that the same systematics for $N_{\rm r}$ seems to be valid for tightly bound nuclei like ^{12}C and ^{16}O as well. It is hard to imagine that the breakup couplings have the same effects for both weakly and tightly bound nuclei. One question one may ask is how sensitive are the elastic scattering and total reaction cross sections of tightly bound nuclei to the optical potential parameters? If they were not sensitive to the potential parameters, this would solve the puzzle and it would suggest that the optical model potentials cannot be determined well for tightly bound heavy nuclei. We check the sensitivity of the angular distributions of differential cross sections and the total reaction cross sections to the four potential parameters in our single-folding model; namely $N_{\rm r}$, $N_{\rm i}$, $t_{\rm r}$, and $t_{\rm i}$. We study this problem with ^{12}C elastic scattering from ^{208}Pb at 85 and 480 MeV. We take the results with the systematic potentials, namely, $N_{\rm r}$ and $N_{\rm i}$ given by Eqs. (3) and (4), respectively, and $t_{\rm r} = 1.25$ fm and $t_{\rm i} = 1.35$ fm as the benchmark and check the changes in elastic scattering angular distributions (taking χ^2 as the criterion) and in total reaction cross section (by percent) with respect to the changes of these parameters. For each parameter a multiplication factor varying from 0.5 to 1.5 with steps of 0.05 were applied. The χ^2 values were evaluated with $\theta_{\rm c.m.}$ from 20° to 100° for 84.9 MeV and

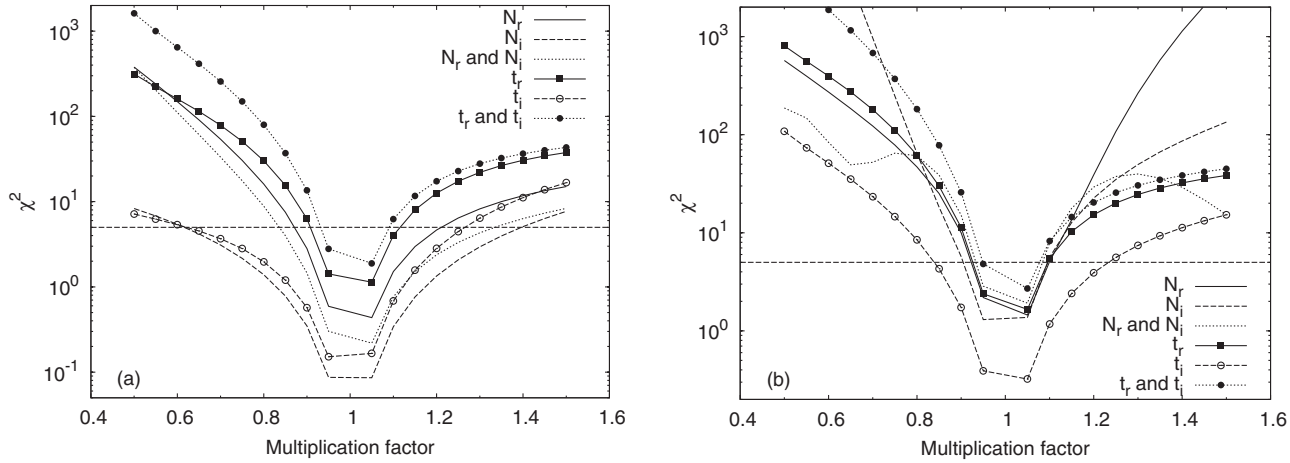

FIG. 12. Sensitivity test of angular distributions of differential cross sections of potential parameters for ^{12}C elastic scattering from ^{208}Pb at (a) 84.9 MeV and (b) 480 MeV. The curves are for renormalization factors, and the curves with symbols are for finite-range Gaussian parameters.

from 4° to 24° for the 480 MeV case assuming a uniform 10% uncertainty for the ratio-to-Rutherford cross sections at each scattering angle. The result is shown in Fig. 12. One sees that, at lower energies, the angular distribution data is more sensitive to the changes in the real part of the potential, both in N_r and t_r, while at 480 MeV sensitivity to changes in N_i becomes equally important. Actually, the lower sensitivity in t_i has been found in studies of α-particle scattering [9]. If we take $\chi^2 = 5$ (averaged by number of angular points) as a criterion of "acceptable agreement," we see that angular distribution data can confine N_r values within 20% and t_r values within around 15% at 84.9 MeV and these confinements are stronger at 480 MeV. The total reaction cross sections, on the other hand, are more sensitive to the changes in the parameters of the imaginary potentials; namely N_i and t_i, and depend very weakly on N_r and t_r. Figure 13 suggests that if the total reaction cross sections were measured with 5% error bars, they can confine the N_i values within about 20% and the t_i values within about 15%. These uncertainties are consistent with the uncertainties we get in Eqs. (3) and (4). It is now clear, with the above criteria, that the potential parameters can be determined with uncertainties smaller than the needed renormalization of folding-model potentials for ^{6}Li caused by breakup-coupling effects. More efforts should be made to better understand these phenomena.

IV. SUMMARY

Elastic scattering of ^{6}Li from heavy targets at incident energies between 5 and 40 MeV was analyzed with a single-folding model. The simple energy dependence of the potential parameters was obtained [Eqs. (3) and (4)], which was found to reproduce the angular distributions of elastic scattering cross sections and total reaction cross sections for projectiles with atomic masses up to around $A = 40$, including both stable and unstable nuclei, for peripheral collisions without strong-coupling effects (e.g., Coulomb excitations or projectile breakup couplings) to the elastic scattering channel. This result suggests that a global nucleus-nucleus potential can be achieved with the single-folding model based on

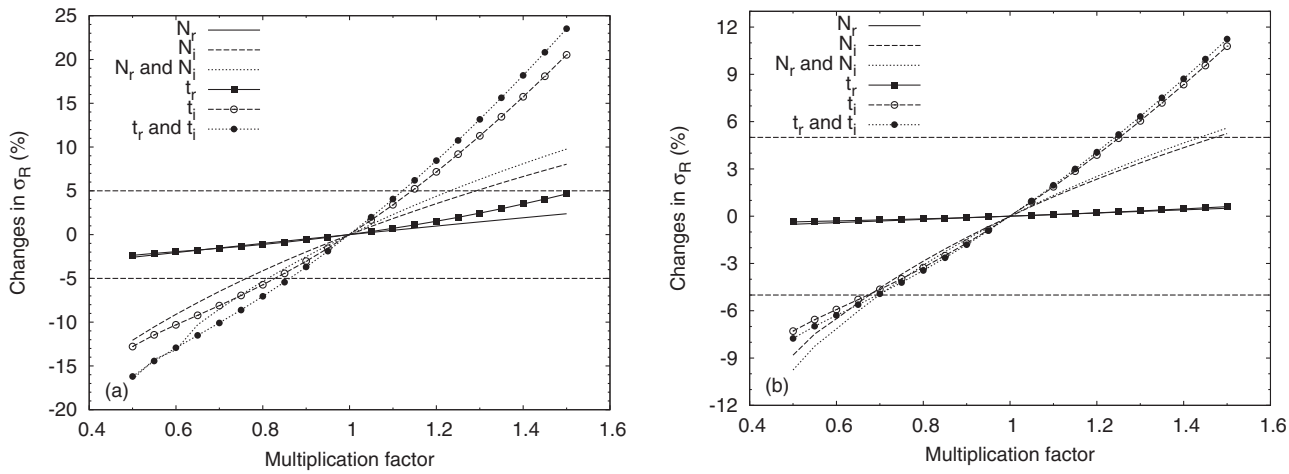

FIG. 13. Same as Fig. 12 but for total reaction cross sections.

the JLMB model of systematic nucleon-nucleus potentials and reasonable nucleon density distributions of the colliding nuclei. Further analysis including more experimental data for heavier projectiles will be made for the proposed global nucleus-nucleus potential. Theoretical efforts should also be made to understand the amplitudes and the energy dependence of renormalization factors for these single-folding heavy-ion potentials.

ACKNOWLEDGMENTS

D.Y.P. thanks Professor R. S. Mackintosh for comments and suggestions. This work is supported by the the National Natural Science Foundation of China under Grants No. 11275018, No. 11021504, and No. 11035001, and by the Research Fund for the Doctoral Program of Higher Education of China (Grant No. 20121102120026).

[1] X. D. Liu, M. A. Famiano, W. G. Lynch, M. B. Tsang, and J. A. Tostevin, Phys. Rev. C **69**, 064313 (2004).
[2] F. D. Becchetti, Jr. and G. W. Greenlees, Phys. Rev. **182**, 1190 (1969).
[3] R. L. Varner, W. J. Thompson, T. L. McAbee, E. J. Ludwig, and T. B. Clegg, Phys. Rep. **201**, 57 (1991).
[4] A. J. Koning and J. P. Delaroche, Nucl. Phys. A **713**, 231 (2003).
[5] W. W. Daehnick, J. D. Childs, and Z. Vrcelj, Phys. Rev. C **21**, 2253 (1980).
[6] F. D. Becchetti, Jr. and G. W. Greenlees, in *Polarization Phenomena in Nuclear Reactions*, edited by H. H. Barschall and W. Haeberli (The University of Wisconsin Press, Madison, 1971), p. 682.
[7] D. Y. Pang, P. Roussel-Chomaz, H. Savajols, R. L. Varner, and R. Wolski, Phys. Rev. C **79**, 024615 (2009).
[8] Xiaohua Li, Chuntian Liang, and Chonghai Cai, Nucl. Phys. A **789**, 103 (2007).
[9] D. Y. Pang, Y. L. Ye, and F. R. Xu, Phys. Rev. C **83**, 064619 (2011).
[10] J. Cook, Nucl. Phys. A **388**, 153 (1982).
[11] G. R. Satchler, *Direct Nuclear Reactions* (Oxford University Press, New York, 1983).
[12] L. C. Chamon *et al.*, Phys. Rev. C **66**, 014610 (2002).
[13] E. Crema, L. C. Chamon, and P. R. S. Gomes, Phys. Rev. C **72**, 034610 (2005).
[14] J. M. B. Shorto, P. R. S. Gomes, J. Lubian, L. F. Canto, S. Mukherjee, and L. C. Chamon, Phys. Lett. B **678**, 77 (2009).
[15] T. Furumoto, W. Horiuchi, M. Takashina, Y. Yamamoto, and Y. Sakuragi, Phys. Rev. C **85**, 044607 (2012).
[16] D. G. Perkin, A. M. Kobos, and J. R. Rook, Nucl. Phys. A **245**, 343 (1975).
[17] D. F. Jackson and R. C. Johnson, Phys. Lett. B **49**, 249 (1974).
[18] D. Y. Pang, Y. L. Ye, and F. R. Xu, J. Phys. G **39**, 095101 (2012).
[19] E. Bauge, J. P. Delaroche, and M. Girod, Phys. Rev. C **58**, 1118 (1998).
[20] E. Bauge, J. P. Delaroche, and M. Girod, Phys. Rev. C **63**, 024607 (2001).
[21] G. R. Satchler, Nucl. Phys. A **329**, 233 (1979).
[22] D. T. Khoa, H. S. Than, T. H. Nam, M. Grasso, and N. Van Giai, Phys. Rev. C **69**, 044605 (2004).
[23] B. A. Brown, Phys. Rev. C **58**, 220 (1998).
[24] B. A. Brown, W. A. Richter, and R. Linsday, Phys. Lett. B **483**, 49 (2000).
[25] B. A. Brown, S. Typel, and W. A. Richter, Phys. Rev. C **65**, 014612 (2001).
[26] W. A. Richter and B. A. Brown, Phys. Rev. C **67**, 034317 (2003).
[27] Jenny Lee, J. A. Tostevin, B. A. Brown, F. Delaunay, W. G. Lynch, M. J. Saelim, and M. B. Tsang, Phys. Rev. C **73**, 044608 (2006).
[28] F. Petrovich, D. Stanley, L. A. Parks, and P. Nagel, Phys. Rev. C **17**, 1642 (1978).
[29] Experimental Nuclear Reaction Data (EXFOR/CSISRS)[DB(DB/OL)] [http://www.nndc.bnl.gov/exfor/exfor00.htm].
[30] L. T. Chua, F. D. Becchetti, J. Jänecke, and F. L. Milder, Nucl. Phys. A **273**, 243 (1976).
[31] P. Schwandt, W. W. Jacobs, M. D. Kaitchuck, P. P. Singh, W. D. Ploughe, F. D. Becchetti, and J. Jänecke, Phys. Rev. C **24**, 1522 (1981).
[32] J. Cook, H. J. Gils, H. Rebel, Z. Majka, and H. Klewe-Nebenius, Nucl. Phys. A **388**, 173 (1982).
[33] P. D. Clark, T. R. Ophel, J. Nurzynski, C. H. Atwood, and D. F. Hebbard, Nucl. Phys. A **352**, 267 (1981).
[34] I. J. Thompson, Comput. Phys. Rep. **7**, 167 (1988).
[35] F. James and M. Roos, Comput. Phys. Commun. **10**, 343 (1975).
[36] A. Nadasen, M. McMaster, M. Fingal *et al.*, Phys. Rev. C **39**, 536 (1989).
[37] Krishichayan, X. Chen, Y. W. Lui, J. Button, and D. H. Youngblood, Phys. Rev. C **81**, 044612 (2010).
[38] K. D. Veal, C. R. Brune, W. H. Geist *et al.*, Phys. Rev. C **60**, 064003 (1999).
[39] R. Huffman, A. Galonsky, R. Markham, and C. Williamson, Phys. Rev. C **22**, 1522 (1980).
[40] Yu. A. Glukhov, A. S. Demyanova, V. I. Manko *et al.*, *Inst. Atomnoy Energii*, Kurchatov Reports IAE-2989 (1978).
[41] R. Wadsworth, M. D. Cohler, M. J. Smithson *et al.*, J. Phys. G: Nucl. Phys. **9**, 1237 (1983).
[42] D. J. Horen, R. L. Auble, J. G. D. Campo *et al.*, Phys. Rev. C **47**, 629 (1993).
[43] X. Chen, Y. W. Lui, H. L. Clark, Y. Tokimoto, and D. H. Youngblood, Phys. Rev. C **76**, 054606 (2007).
[44] K. Becker, K. Blatt, H. J. Jansch *et al.*, Nucl. Phys. A **535**, 189 (1991).
[45] J. M. Figueira, J. O. Fernández Niello, A. Arazi *et al.*, Phys. Rev. C **81**, 024613 (2010).
[46] Zhang Chun-Lei, Zhang Huan-Qiao, Lin Cheng-Jian *et al.*, Chin. Phys. Lett. **23**, 1146 (2006).
[47] N. Keeley, S. J. Bennett, N. M. Clarke *et al.*, Nucl. Phys. A **571**, 326 (1994).
[48] N. Keeley, J. M. Cook, K. W. Kemper, B. T. Roeder, W. D. Weintraub, F. Marechal, and K. Rusek, Phys. Rev. C **68**, 054601 (2003).
[49] S. Santra, V. V. Parkar, K. Ramachandran *et al.*, Phys. Lett. B **677**, 139 (2009).
[50] C. W. Glover, R. I. Cutler, and K. W. Kemper, Nucl. Phys. A **341**, 137 (1980).
[51] M. F. Steeden, J. Coopersmith, S. J. Cartwright, M. D. Cohler, N. M. Clarke, and R. J. Griffiths, J. Phys. G: Nucl. Phys. **6**, 501 (1980).
[52] D. Gupta, C. Samanta, R. Kanungo *et al.*, Nucl. Phys. A **646**, 161 (1999).

[53] D. Gupta, C. Samanta, A. Chatterjee *et al.*, Nucl. Phys. A **683**, 3 (2001).
[54] A. F. Zeller, D. C. Weisser, T. R. Ophel, and D. F. Hebbard, Nucl. Phys. A **332**, 515 (1979).
[55] D. Y. Pang and R. S. Mackintosh, Phys. Rev. C **84**, 064611 (2011).
[56] Dao T. Khoa, W. von Oertzen, H. G. Bohlen, and S. Ohkubo, J. Phys. G: Nucl. Phys. **34**, R111 (2007).
[57] G. R. Satchler, Phys. Lett. B **59**, 121 (1975).
[58] P. Roussel-Chomaz *et al.*, Nucl. Phys. A **477**, 345 (1988).
[59] C. Mahaux, H. Ngô, and G. R. Satchler, Nucl. Phys. A **449**, 354 (1986).
[60] L. C. Chamon, D. Pereira, M. S. Hussein, M. A. Cândido Ribeiro, and D. Galetti, Phys. Rev. Lett. **79**, 5218 (1997).
[61] H. Kumawat, V. Jha, B. J. Roy, V. V. Parkar, S. Santra *et al.*, Phys. Rev. C **78**, 044617 (2008).
[62] M. Biswas, Subinit Roy, M. Sinha, M. K. Pradhan, A. Mukherjee *et al.*, Nucl. Phys. A **802**, 67 (2008).
[63] N. N. Deshmukh, S. Mukherjee, D. Patel, N. L. Singh, P. K. Rath *et al.*, Phys. Rev. C **83**, 024607 (2011).
[64] B. M. Oginni, S. M. Grimes, A. V. Voinov, A. S. Adekola, C. R. Brune *et al.*, Phys. Rev. C **80**, 034305 (2009).
[65] A. Shrivastava, A. Navina, N. Keeley, K. Mahata, K. Ramachandran *et al.*, Phys. Lett. B **633**, 463 (2006).
[66] M. D. L. Barbosa, T. Borello-Lewin, L. B. Horodynski-Matsushigue, J. L. M. Duarte, C. L. Rodrigues, M. R. D. Rodrigues, and G. M. Ukita, Phys. Rev. C **71**, 024303 (2005).
[67] F. A. Souza, N. Carlin, C. Beck, N. Keeley, A. Diaz-Torres *et al.*, Eur. Phys. J. A **44**, 181 (2010).
[68] L. Fimiani, J. M. Figueira, G. V. Mart, J. E. Testoni, A. J. Pacheco *et al.*, Phys. Rev. C **86**, 044607 (2012).
[69] V. V. Parkar, V. Jha, B. J. Roy, S. Santra, K. Ramachandran, A. Shrivastava, A. Chatterjee, S. R. Jain, A. K. Jain, and S. Kailas, Phys. Rev. C **78**, 021601(R) (2008).
[70] S. Kox, A. Gamp, C. Perrin, J. Arvieux, R. Bertholet *et al.*, Phys. Rev. C **35**, 1678 (1987).
[71] L. W. Townsend and J. W. Wilson, Phys. Rev. C **37**, 892 (1988).
[72] D. T. Khoa, Phys. Rev. C **63**, 034007 (2001).
[73] G. R. Satchler, Nucl. Phys. A **540**, 533 (1992).
[74] S. Santra, P. Singh, S. Kailas, A. Chatterjee, A. Shrivastava, and K. Mahata, Phys. Rev. C **64**, 024602 (2001).
[75] F. Videbaek, R. B. Goldstein, L. Grodzins, S. G. Steadman, T. A. Belote, and J. D. Garrett, Phys. Rev. C **15**, 954 (1977).
[76] A. M. Stefanini, A. Tivelli, G. Montagnoli, D. R. Napoli, D. Bonamini *et al.*, Phys. Rev. C **41**, 1018 (1990).
[77] D. M. Herrick, F. L. H. Wolfs, D. C. Bryan, C. G. Freeman, K. L. Kurz, D. H. Mathews, P. A. A. Perera, and M. T. Zanni, Phys. Rev. C **52**, 744 (1995).
[78] B. Bilwes, R. Bilwes, J. Diza, and J. L. Ferrero, Nucl. Phys. A **449**, 519 (1986).
[79] N. Alamanos, F. Auger, J. Barrette, B. Berthier, B. Fernandez, J. Gastebois, and L. Papineau, Phys. Lett. B **137**, 37 (1984).
[80] Y. Y. Yang *et al.* [Phys. Rev. C (to be published)] (2013).
[81] Y. Y. Yang (private communication).
[82] J. F. Liang, J. R. Beene, A. Galindo-Uribarri, C. J. Gross, P. A. Hausladen *et al.*, Phys. Rev. C **67**, 044603 (2003).
[83] J. F. Liang, J. R. Beene, H. Esbensen, A. Galindo-Uribarri, J. Gomez del Campo *et al.*, Phys. Rev. C **65**, 051603(R) (2002).
[84] M. G. Saint-Laurent, R. Anne, D. Bazin, D. Guillemaud-Mueller, U. Jahnke *et al.*, Zeitschrift für Physik A Atomic Nuclei **332**, 457 (1989).
[85] E. Liatard, J. F. Bruandet, F. Glasser, S. Kox, Tsan Ung Chan *et al.*, Europhys. Lett. **13**, 401 (1990).
[86] J. F. Bruandet, J. Phys., Colloq. **47**, 125 (1986).
[87] L. Acosta, A. M. Sánchez-Benítez, M. E. Gómez, I. Martel *et al.*, Phys. Rev. C **84**, 044604 (2011).
[88] A. Di Pietro, G. Randisi, V. Scuderi, L. Acosta, F. Amorini *et al.*, Phys. Rev. Lett. **105**, 022701 (2010).
[89] A. Di Pietro, V. Scuderi, A. M. Moro, L. Acosta, F. Amorini *et al.*, Phys. Rev. C **85**, 054607 (2012).
[90] S. Szilner, L. Corradi, G. Pollarolo, S. Beghini, B. R. Behera *et al.*, Phys. Rev. C **71**, 044610 (2005).
[91] Jiang Cheng-Lie, P. R. Christensen, O. Hansen, S. Pontoppidan, F. Videbaek, D. Schüll, Shen Wen-Qing, A. J. Baltz, P. D. Bond, H. Freiesleben, F. Busch, and E. R. Flynn, Phys. Rev. Lett. **47**, 1039 (1981).
[92] G. R. Satchler and W. G. Love, Phys. Rep. **55**, 183 (1979).
[93] Yukinori Sakuragi, Masanobu Yahiro, and Masayasu Kamimura, Prog. Theor. Phys. Suppl. **89**, 136 (1986).